SCIENCE CHINA
Chemistry

• ARTICLES •
• SPECIAL ISSUE • Recent Research Progress of Biomedical Polymers

April 2014 Vol.57 No.4: 596–604
doi: 10.1007/s11426-013-4997-3

Surface patterning and modification of polyurethane biomaterials using silsesquioxane-gelatin additives for improved endothelial affinity

HOU LinXi[1,2,†,*], PECK Yvonne[2†], WANG XiaoWen[1] & WANG DongAn[2*]

[1]*College of Chemistry and Chemical Engineering, Fuzhou University, Fuzhou 350108, China*
[2]*Division of Bioengineering, School of Chemical and Biomedical Engineering, Nanyang Technological University, Singapore 637457, Singapore*

Received June 7, 2013; accepted July 25, 2013; published online October 30, 2013

Polyurethanes (PUs) are well-known for their biocompatibility but their intrinsic inert property hampers cell-matrix interactions. Surface modifications are thus necessary to widen their use for biomedical applications. In this work, surface modifications of PU were achieved first by incorporating polyhedral oligomeric silsesquioxane (POSS), followed by alteration of the surface topography via the breath figures method. Subsequently, surface chemistry was also modified by immobilization of gelatin molecules through grafting, for the enhancement of the surface cytocompatibility. Scanning electron microscopy (SEM) was used to verify the formation of highly ordered microstructures while static contact angle, FTIR and XPS confirmed the successful grafting of gelatin molecules onto the surfaces. *In vitro* culture of human umbilical vein endothelial cells (HUVECs) revealed that endothelial cell adhesion and proliferation were significantly enhanced on the gelatin-modified surfaces, as shown by live/dead staining and WST-1 proliferation assay. The results indicated that the combination of the strategies yielded an interface that improves cell attachment and subsequent growth. This enhancement is important for the development of higher quality biomedical implants such as vascular grafts.

biomaterials, surface modification, pattern, polyurethane, silsesquioxane, gelatin, endothelization

1 Introduction

Cardiovascular diseases (CVDs) have resulted in over millions of vascular procedures, including bypass graftings performed annually [1]. The most common approach for these procedures is to use autologous blood vessels harvested from patients for transplantation. However, limited availability of healthy autologous blood vessels for grafting has necessitated the use of various synthetic vascular grafts [2, 3]. Some of the more commonly used polymeric materials for this purpose are polyurethane (PU) [4, 5], polyethylene terephthalate (PET), polytetrafluoroethylene (PTFE) [6], polyvinyl chloride (PVC), silicon rubber, and so on [7]. Among them, PU remains one of the most popularly used materials for the construction of vascular grafts due to its excellent mechanical and physical properties [8]. However, as with other synthetic vascular grafts, PU-based vascular grafts have been associated with poor long-term antithrombogenicity [9, 10]. This is presumably caused by inadequate endothelization [11]. In order to overcome this problem, a monolayer of functional endothelial cells can be created on the graft surface to improve endothelization [12]. In recent years, researchers have developed a new class of silica nanocomposites using polyhedral oligomeric silsesquioxane (POSS). POSS has been recognized as a nanosized silica particle with great potential for use in cardiovascular interventional devices [13]. Some studies have

†These authors contributed equally to this work
*Corresponding authors (email: lxhou@fzu.edu.cn; DAWang@ntu.edu.sg)

shown that POSS molecules are able to act as amphiphiles at water-air interface, thus their incorporation into a polymer would enhance the amphilicity of a surface. This would in turn improve endothelization. In fact, there are many reports that have shown the high biocompatibility, nontoxicity and good cytocompatibility of POSS nanocomposites, indicating that the combination of the unique POSS molecules and polymers holds great promise, especially as biomaterials used for biomedical applications [14].

Besides selecting suitable biomaterials for the construction of vascular grafts, surface modifications are also essential to enhancing the viability of endothelial cells on the graft surfaces [15, 16]. Recently, a bottom-up approach known as the breath-figure (BF) technique has become an important alternative to the conventional top-down templating strategy such as photolithography to produce microporous polymer films with highly ordered structures. This technique was first introduced by Francois *et al*. [17, 18] and is based on the *in situ* condensation of water droplets onto a drying polymer solution surface. It is a relatively simple templating method where the films are produced from simple casting of a volatile solvent onto a flat surface in a highly humid environment. The cooling effect from rapid solvent evaporation will then cause condensation and the formation of water droplets to occur. These water droplets are capable of self-assembling into hexagonally packed arrays, forming highly ordered honeycomb-structured films. The popularity of this method comes from the fact that it is easily manipulated, low-cost, applicable to large area fabrication, and most importantly, the consistency of the array of holes formed and the average pore size of the porous films produced by this method are tunable. To date, various block copolymers and homopolymers, either with or without the use of surfactants, have been utilized for the fabrication of exquisite arrays of holes [18].

Besides introducing microstructures onto the polymer surfaces to modify the surface topology, surfaces can also be modified or functionalized by immobilizing biomacromolecules. Some studies have described the immobilization of different biomacromolecules such as gelatin, biotin or RGD peptides onto the polymeric material surfaces to improve cell-material interactions [19–25]. In particular, gelatin has been shown to be effective in the enhancement of cell attachment properties on a PU surface [26].

In this study, we report the development of gelatin-grafted PU/POSS membranes with highly ordered, self-organized honeycomb microstructures and enhanced cytocompatibility using the simple but effective breath figures (BF) method. It is a culmination of a two-pronged strategy, which employs the BF method to modify the surface topography of PU (Figure 1) and the incorporation of POSS and gelatin molecules to enhance the endothelization of PU so as to improve its long-term anti-thrombogenicity (Figure 2). A variety of surface characterization techniques were used to verify the formation of highly ordered microstructures and the successful grafting of gelatin molecules onto the surfaces. Additionally, this study also verified previous findings that detailed the possibility of fine-tuning these microstructures by controlling the various parameters such as solvent type and polymer concentration during synthesis [27]. Furthermore, the effectiveness of these surface modifications on improving the endothelization of PU was also confirmed by the culturing of human umbilical vein endothelial cells (HUVECs) on films and accessing their viability and proliferation through Live/Dead staining and WST-1 proliferation assay. The effect of pore size on cell attachment and growth was also probed.

2 Experimental

2.1 Materials

PU, with a molecular weight of M_w = 106500, is an aromatic polyester-based thermoplastic polyurethane purchased from

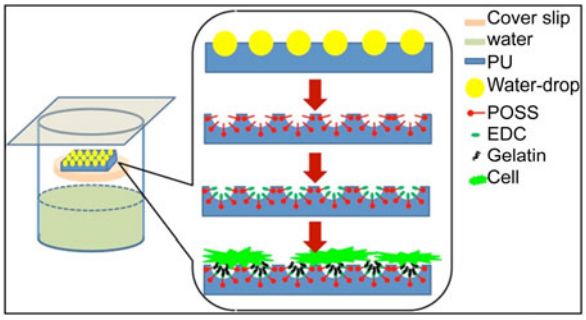

Figure 1 Schematic diagram showing the preparation of a honeycomb-structured gelatin-grafted PU/POSS film via the BF method.

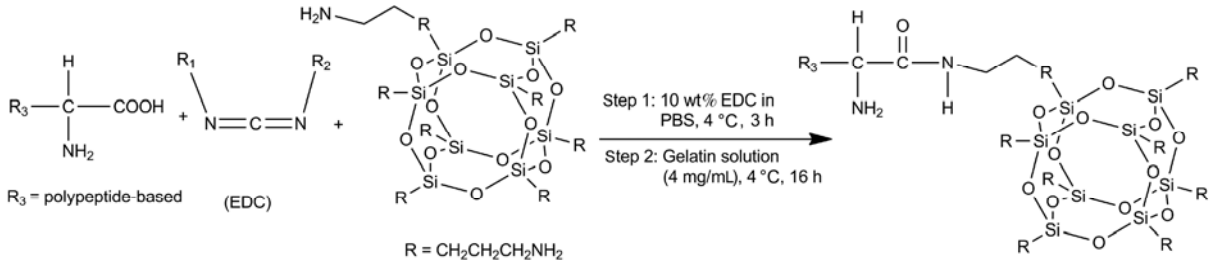

Figure 2 Gelatin grafting reactions in the pores of PU/POSS films.

Noveon. The aminopropyl isobutyl polyoligomeric silsesquioxane (POSS–trademark of hybrid plastics, AM0265) was purchased from Hybrid Plastics. The chloroform was obtained from Fisher Scientific and used without further purification. Furthermore, the cross-linking agent, *N*-(3-dimethylaminopropyl)-*N*′-ethylacarbodiimide hydrochloride (EDC. HCl) and gelatin were purchased from Sigma-Aldrich and used as received. Dulbecco's phosphate buffered saline (DPBS, 1 x) was obtained from Invitrogen and water used throughout this study was purified by a millipore system (Milli-Q, millipore).

2.2 PU/POSS microporous film preparation

The microporous films of PU and POSS molecules were prepared by using the static BF method, which is relatively simpler as compared to the typical dynamic BF process [28]. The POSS concentration was fixed at 1 mg/mL. Briefly, a predetermined amount of PU and POSS were weighed and added into chloroform, and mixed to achieve homogeneous mixture solution in an ultrasonic field for 10 hours. Then, 40 μL of the homogenously-mixed solution was cast onto a glass coverslip using a pipette in a self-made humidified chamber at room temperature (23 °C) and a preset relative humidity of 90% RH, and left inside for at least 45 minutes. When the organic solvent and water have fully evaporated, the polymer films on the glass coverslip were retrieved for additional treatment. A number of uniform circular sections, each measuring 16 mm in diameter, were cut out and placed into the wells of a 24-well cell culture plate. Each well containing the films was later filled with 1 mL of PBS containing 10 wt% of EDC and the plate was kept in the refrigerator at 4 °C for 3 hours. Subsequently, a gelatin solution (4 mg/mL) was used to replace the EDC solution and kept for another 16 hours in the refrigerator at 4 °C. In parallel, other spin-coated flat-surface films were also prepared to be used as the control.

2.3 Stability of POSS in PU

To examine the stability of the POSS additives in PU films, polymer films were cut into 16 mm diameter circular sections and weighed (W_{dry}) before being immersed in phosphate buffer solution (PBS) under pH 7.4 at 37 °C for 20 days. After aging, the test samples were thoroughly cleaned with ethanol and subsequently rinsed with deionised water. The samples were then left in the vacuum oven to dry for 12 hours at 80 °C before being weighed again ($W_{dry, final}$). The extraction of the additives in terms of weight loss from the films was determined by the following equation [29]:

$$\text{Weight loss } (\%) = \frac{W_{dry} - W_{dry,\ final}}{W_{dry}} \times 100.$$

2.4 Polymer characterization

The honeycomb films were characterized and observed using an optical microscope (BX-90, Olympus). Attenuated total reflectance-Fourier transform infrared (ATR-IR) spectra were obtained on a Nicolet Magna- IR9300 FTIR spectrometer. The morphology of the honeycomb films was observed and images were taken on a scanning electron microscope (JSM6700F, JOEL, Japan). The contact angles of pure water on the surface of the films were measured at room temperature on a KH-0601 optical contact angle-testing instrument (Kangsente, Beijing, China) and evaluated using the Dropshape software (Kruess, Germany). NMR spectra of the compounds were recorded on a Bruker 400 MHz NMR Spectrometer using DMSO-d6 as solvent. The surface chemical composition of the films was analyzed with X-ray photoelectron spectroscopy (XPS) (Kratos, Manchester, UK).

2.5 Cell culture

Human umbilical vein endothelial cells (HUVECs) were purchased from American Type Culture Collection (ATCC). HUVECs were cultured in MCDB 131 medium supplemented with 10% fetal bovine serum (Hyclone), 20 units/mL heparin, 1 mM sodium pyruvate, 100 units/mL penicillin, and 100 mg/mL streptomycin. Cells were maintained at 37 °C in a humidified atmosphere of 5% CO_2 in air and were subcultured until approximately 80% confluent before they were trypsinized for further use. HUVECs below passage 10 were used for this study.

2.6 *In vitro* cytocompatibility

For *in vitro* cytocompatibility studies, the PU/POSS films were cut into 16 mm diameter circular sections. The circular scaffolds were sterilized by being immersed in Penicillin/Streptomycin (10x) (PAA) overnight and then washed thoroughly by phosphate buffered saline (PBS) (Invitrogen). HUVECs cultured in 175 cm^2 cell culture flasks were trypsinized, counted, and seeded at a density of 1×10^4 cells/cm^2 onto the surface of the pre-prepared scaffolds that were placed in 24-well cell culture plates. Cell-seeded scaffolds were incubated at 37 °C for 2 hours to allow HUVECs to attach to the scaffolds before the topping up each well with 1 mL of culture medium. After culturing for a week, the PU/POSS scaffolds were harvested, washed with PBS to remove the non-adherent cells and then Live/Dead fluorescent staining (Invitrogen) was performed. The live (stained green) and dead (stained red) cells were observed under a fluorescent microscope after 30 minutes of incubation with the fluorescent dyes and thorough wash with PBS.

Besides that, cell proliferation on both gelatin-grafted PU/POSS films and control films was also evaluated using WST-1 proliferation assay (4-[3-(4-Iodophenyl)-2-(4-nitro-

phenyl)-2*H*-5-tetrazolio]-1,3-benzene disulfonate assay, Roche Diagnostics, Germany). HUVEC-seeded films in uniform circular sections (16 mm in diameter) were collected on day 1, 3 and 7. The samples were washed twice in PBS solution, followed by incubation in 300 μL serum-free medium containing 30 μL of WST-1 reagent for 2 hours. The absorbance at 450 nm with 690 nm as reference was measured using a microplate reader (Multiskan spectrum, Thermo).

3 Results and discussion

3.1 Development and characterization of PU/POSS films

In the first part of this work, the synthesis and characterization of gelatin-grafted PU/POSS with highly ordered honeycomb-structured porous films was done. Stability of POSS in PU was tested in PBS. SEM was used to observe and examine the morphology of the honeycomb films while static contact angle measurements, ATR-FTIR, and XPS indicated that the gelatin immobilization onto the surface of the films was successful.

Stability of POSS in PU

The incorporation of POSS into the polyurethane matrix will affect the surface and bulk properties of the PUs. It is important that the POSS molecules are retained in the PU matrix to ensure the integrity of the material. The stability of POSS in PU can be examined by immersing the films in PBS and measuring their weight change at selected time-points over a period of 20 days (as shown in Figure 3). PU/POSS films were shown to experience very minimal weight loss (not exceeding 1%) over the first 12 days of study before becoming stabilized over the remaining 8 days. The weight loss from the PU/POSS films confirms that some of the POSS molecules have leached out of the PU matrix into the bulk media. However, since the loss is very minimal, this indicates that the POSS molecules are reasonably stable in PU when exposed to PBS due to their hydrophobic nature [29].

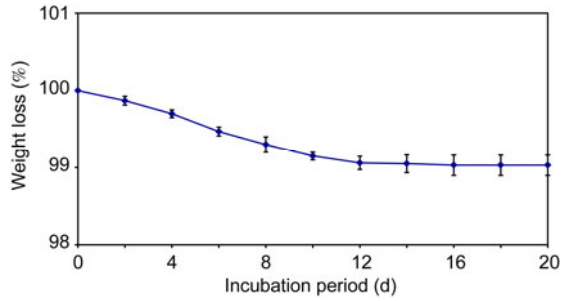

Figure 3 Weight loss of the PU/POSS films at selected time points over a period of 20 days of immersion in PBS at 37 °C.

Morphology of the honeycomb-structured PU/POSS films

The preparation of ordered microporous films using the BF templating strategy has been extensively studied [30–34]. During this procedure, it has been known that the condensation of water vapor resulted in the formation of water droplets that acted as the template for the ordered array of holes. This phenomenon is basically caused by the cooling effect resulting from the evaporation of volatile solvents. The polymers surrounding the water droplets eventually precipitate, forming highly ordered structures. Some of the important parameters that affect the precipitation rate of the polymers are polymer concentration, choice of solvent and the type of polymer used [35]. The use of the various types of volatile solvents in mediating the formation of porous films has been investigated by a number of studies [36, 37]. Different solvents are normally required for the different polymers used. It is well established that the formation of porous structures is very much related to the rate of evaporation of the solvent. A highly evaporative solvent would increase the cooling rate on the surfaces of the polymer solution and thus induce rapid condensation of water vapor [27]. In this work, three different solvents with different vapor pressures were used to probe the effect of solvent types on the microstructures of the PU/POSS porous films, while the PU concentration was kept at 10 mg/mL. This is to determine the optimal solvent type for the synthesis of PU/POSS films with highly ordered structures via the BF route so that these films can be potentially used for biomedical applications.

Figure 4(b–d) shows the SEM pictures of the PU/POSS films formed by using different solvent types at 25 °C. The three different solvents used for the dissolution of PU were toluene, tetrahydrofuran (THF), and chloroform. It is apparent that regardless of the solvent used for film preparation, all the films showed a honeycomb porous structure. However, it was observed that the pore distribution, uniformity in shape and size were affected by the choice of solvent. When toluene was used as a solvent, PU/POSS films with uneven distribution of pores were obtained (Figure 4(b)). Furthermore, the pores formed were not uniformly shaped, where some pores assumed rounded shapes while the rest did not. The pores formed have an average pore size of 7.25 μm. As toluene was replaced with tetrahydrofuran (THF) as a solvent, the films produced were shown to have more evenly distributed pores with more regular shapes and a smaller average pore size (2.27 μm) although the porous structures were still not well-defined (Figure 4(c)). Among these solvents, the PU/POSS films produced using chloroform yielded the most ordered honeycomb structures as evidenced by the regularly shaped and evenly distributed pores (Figure 4(d)). The pore diameters were measured to be in the range of 1.83 to 3.36 μm. The difference in pore distribution, shape and size due to the different solvents can be explained by the difference in their vapor pressure.

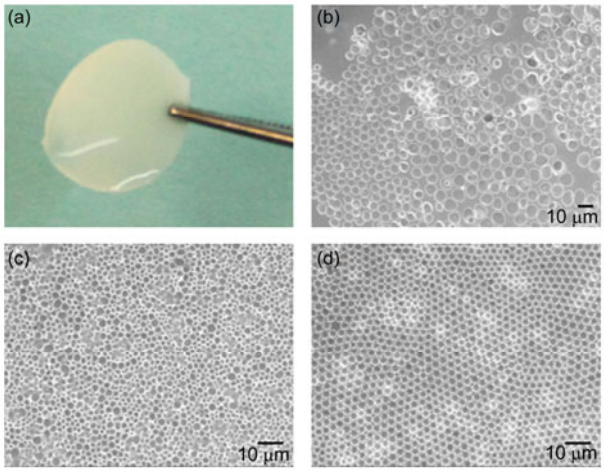

Figure 4 (a) A sample consists of a circular section with a diameter of 16 mm that is cut out from a PU/POSS film. SEM images of the PU/POSS microporous films prepared at room temperature (25 °C) using (b) toluene, (c) THF, (d) chloroform as a solvent. The PU and POSS concentration was kept at 10 and 1 mg/mL, respectively.

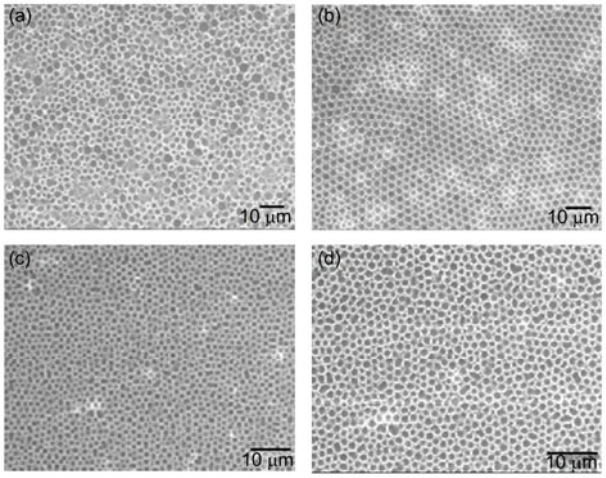

Figure 5 SEM images of the PU/POSS microporous films prepared with a PU concentration of (a) 5, (b) 10, (c) 15, and (d) 20 mg/mL. Chloroform was used as a solvent and the concentration of POSS was fixed at 1mg/mL.

Generally, higher vapor pressure causes the solvent to evaporate at a higher rate [27]. The vapor pressure of toluene is comparable to water at room temperature, while the other two solvents have comparatively much higher vapor pressure. Thus, when toluene was used as a solvent, water condensation occurred at a much lower rate, allowing the self-assembling water droplets to coalesce with one another, partly aided by the presence of the polar amino groups in the POSS molecules. Ultimately, this caused the formation of bigger pores with irregular patterns. Since chloroform has the highest vapor pressure, this would undoubtedly result in the fastest growth of the nucleated water droplets. Therefore, the pores formed were seen to be more well-arranged and smaller in size.

Besides the choice of solvent, the effect of polymer concentration on the porous microstructures was also investigated. The morphology of the PU/POSS microporous films produced with different PU concentrations is shown in Figure 5(a–d). Chloroform was selected as the solvent since it mediated the formation of the most highly ordered structured films. The results show that when the polymer concentration increased from 5 mg/mL (Figure 5(a)), 10 mg/mL (Figure 5(b)), 15 mg/mL (Figure 5(c)) to 20 mg/mL (Figure 5(d)), the average pore size decreased from 3.36 μm to 1.87 μm. This correlation between polymer concentration and pore size is in line with literature [27, 31, 38, 39]. The most ordered array of pores was obtained when the film was prepared at a PU concentration of 10 mg/mL (Figure 5(b)) where the pores are seen to be in an ordered hexagonal arrangement with an average pore size of 2.29 μm. The observed morphological difference between films produced at different PU concentrations can be discussed in terms of difference in the growth rate of water droplets. At higher polymer concentrations, the temperature difference between the atmosphere and the solution surface (ΔT) is smaller due to the lower vapor pressure at the surface of the polymer solution and also the lower rate of evaporation of the solvent. A previous study has shown that the growth rate of water droplets measured by the increase in radius as a function of time (dR/dt) in BF method is affected by ΔT, which is described by $dR/dt \sim \Delta T^{0.8}$ [40]. Therefore, an increase in polymer concentration from 5 mg/mL to 20 mg/mL coincided with a decrease in the growth rate of water droplets. This then led to the formation of water droplets that were smaller in size and ultimately resulted in smaller average pore sizes. In addition to the difference in growth rate, the difference in precipitation rate of PU could have been the cause for the observed morphological differences [27]. At higher polymer concentrations, PU is expected to precipitate at a higher rate, which in turn leads to more efficient encapsulation of the water droplets. This means that solidification occurs almost immediately, leaving insufficient time for the water droplets to grow. Thus, smaller water droplets were formed producing smaller pores such as those films produced at a concentration of 10 mg/mL and 15 mg/mL. Moreover, a higher polymer concentration also corresponds to a higher viscosity, which delays the droplets' growth but promotes and facilitates the encapsulation of condensed water droplets. Consequently, this prevents the water droplets from coalescing, forming a more ordered pattern with smaller average pore sizes [27, 41]. By comparing the results, it was determined that the porous structure produced at a concentration of 10mg/mL is the most ordered which can be due to the right balance among the various contributing parameters such as the vapor pressure, polymer precipitation rate and viscosity.

Physical properties analysis of gelatin-grafted PU/POSS nanocomposites

Contact angle analysis gives important information regard-

ing the surface hydrophilicity of a polymer film, which could serve as an indication of the level of molecular mobility at the surface [29]. A number of studies have shown that surface protein absorption and biocompatibility of a material are affected by surface wettability [42, 43]. As shown in Table 1, the incorporation of POSS molecules into PU has reduced its hydrophilicity as evidenced by an increase in the measured static water contact angle. This is attributed to the presence of the POSS molecules at the surface of the films and more importantly it is related to the hydrophobic nature of POSS. However, after gelatin grafting, the average static water contact angle decreased from a value of 84.6° to 46.6°, indicating an increase in the surface hydrophilicity. This is expected because the surface content is modified by gelatin that contributes a large number of hydroxyl and amino groups to the surface, causing the grafted surface to be more hydrophilic.

From the ATR-FTIR spectrum of the unmodified PU film (Figure 6(c)), the stretching band at 1719 cm^{-1} attributed to the C=O group and the two characteristic absorption peaks at 3330 and 1540 cm^{-1}, belonging to the N–H group in the urethane groups were observed. Furthermore, the benzene and methylene group in PU also display absorption at 1596 and 1462 cm^{-1}, respectively. Another significant absorption peak is also seen at 1699 cm^{-1}, which is contributed by the association of ester and amide groups. Upon mixing with POSS molecules, the presence of these nanostructured molecules at the surface has depressed the absorption of PU. By referring to Figure 6(b), it can be observed that the absorption at 1540, 1596 and 1699 cm^{-1} was clearly depressed. Also, the absorption peak at 3330 cm^{-1} was depressed greatly after the incorporation of POSS molecules. After the PUPOSS films were further modified with gelatin through grafting, the presence of the gelatin mole cules can be confirmed by the presence of the various amide bands contributed by the different amino acid residues in gelatin (Figure 6(a)). Firstly, the previously diminishing peak at 3330 cm^{-1}, which is also known as the amide A band is observed to increase in both its intensity and width. This is due to the N–H stretching vibrations in gelatin. Additionally, the amide II absorption (δ N–H) between 1520–1560 cm^{-1} also increased upon grafting with gelatin due to the coupling of the bending of the N–H bond and the stretching of the C–N bond. Furthermore, a number of peaks appeared in the 1400–1200 cm^{-1} region, which corresponds to the amide III region. The presence of these peaks is caused by N–H bending in gelatin [44, 45].

For further verification of the successful grafting of gelatin molecules onto the PUPOSS film surfaces, X-ray photoelectron spectroscopy (XPS) was also employed to analyze the chemical composition differences between unmodified and surface-modified films. The results are shown in Figure 7, where the peaks at 284, 398 and 532 eV in the spectra were assigned to Carbon (C 1s), Nitrogen (N 1s) and oxygen (O 1s), respectively. The elemental composition of the films is summarized in Table 2. It can be seen that upon mixing with POSS molecules, which are rich in Si–O groups, the O/C ratio increased significantly as compared to the unmodified PU films. After the PUPOSS films were grafted with gelatin, the percentage of nitrogen increased from 1.03% to 2.57%. This increase in nitrogen is more apparent when comparing the N/C ratio before and after grafting, where the ratio increased more than double from 0.015 to 0.035. It is hypothesized that the low percentage of nitrogen recorded in the surface of the films is attributed to the minute amount of POSS used in the experiment, which

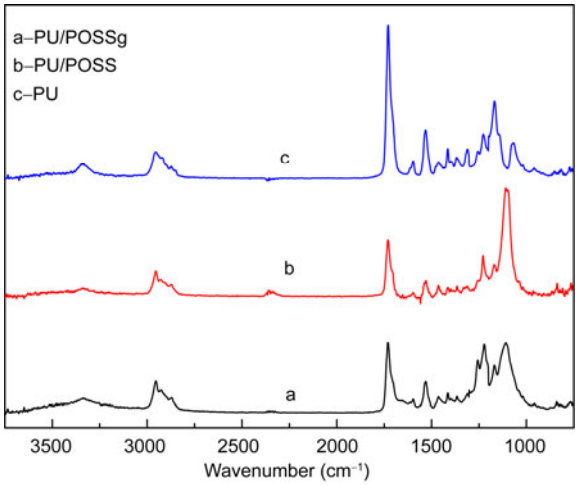

Figure 6 ATR-FTIR spectra of (a) a gelatin-grafted PU/POSS film (PUPOSSg), (b) a POSS-modified PU film (PUPOSS), and (c) an unmodified PU film (PU).

Table 1 Static water contact angle on an unmodified PU film (PU), a POSS-modified PU film (PUPOSS), and a gelatin-grafted PU/POSS (PUPOSSg) film

Samples	PU	PUPOSS	PUPOSSg
Static water contact angle (°)	64.3 ± 1.9	84.6 ± 1.2	46.6 ± 0.9

Table 2 XPS analysis of PU, PU/POSS and gelatin-grafted PU/POSS films

Samples	O	N	C	O/C	N/C
PU	23.9	0.76	75.34	0.317	0.010
PUPOSS	27.99	1.03	70.98	0.394	0.015
PUPOSSg	24.86	2.57	72.57	0.343	0.035

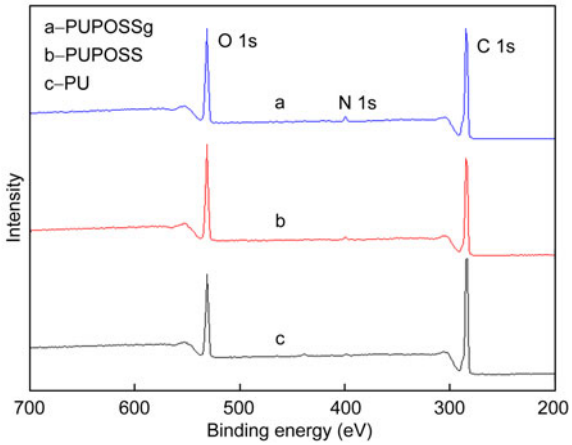

Figure 7 XPS spectra of (a) a gelatin-grafted PU/POSS film (PUPOSSg), (b) a POSS-modified PU film (PUPOSS), and (c) an unmodified PU film (PU).

is as low as 1 mg/mL. It can also be due to the thickness of the grafted gelatin layer that is lower than the sampling depth of XPS.

3.2 Cytocompatibility

The cytocompability of the gelatin-grafted PU/POSS microporous films was investigated by seeding human umbilical vein endothelial cells (HUVECs) onto the films and subsequently examining their adhesion and growth on the films, both qualitatively and quantitatively. The qualitative results from Live/Dead staining on day 7 (Figure 8) revealed that almost no cell adhesion was observed on the surface of the control sample, which is made up of spin-coated PUPOSS films (Figure 8(e)) whereas all the modified surfaces showed enhanced cell adhesion and cell growth properties as evidenced by the attachment and proliferation of the cells over several days. This observation corresponds to the results obtained from the quantitative WST-1 proliferation assay (Figure 9) where all modified groups consistently showed significantly higher cellular proliferative activity as compared to the control group throughout a week of culture. Also, HUVECs seeded on the control surfaces did not show any detectable increase in their proliferative activity after being cultured for a week whereas cells in all other groups remain viable and proliferate well as indicated by the increase in the absorbance values from day 1 to day 7. Additionally, it was observed from the staining images that the cells on modified surfaces mostly showed the typical spread morphology of healthy cells. This is in line with previous studies that have shown that modifications on PU are necessary for the enhancement of cell-material interactions [15, 16, 26, 46–49]. This is because it has long been known that certain topographic features greatly affect the morphological appearance and functional behaviors of cells, which enable them to thrive better [50].

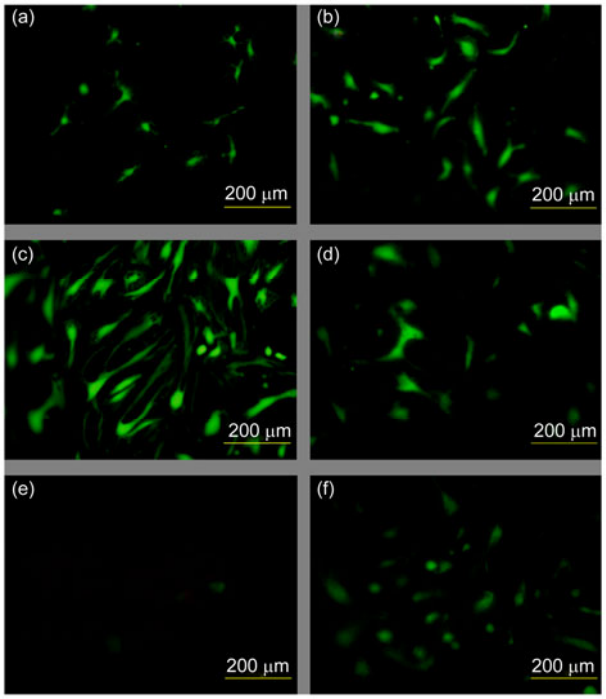

Figure 8 Cytocompatibility of the gelatin-grafted microporous PU/POSS films shown by Live/Dead staining of HUVEC cells at different PU concentration: (a) 5, (b) 10, (c) 15, (d) 20 mg/mL, (f) PU-Pluronic films, while (e) represents the control surface of PU films formed by spin-coating.

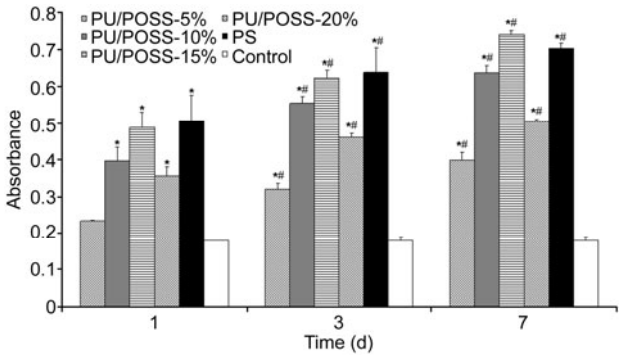

Figure 9 Assessment of cell proliferative activity via WST-1 assay. * indicates $p < 0.05$, significantly different from the control group at day 1, 3 and day 7, respectively; # indicates $p < 0.05$, significantly different from each of the respective group on day 1.

Additionally, it has also been suggested that pore size affects cell adhesion and cell growth [51, 52]. In order to determine the effect of pore size on cellular behaviors, HUVECs were seeded on films with different pore sizes. The pore size of the films was tuned by using different PU concentrations as described in the previous section. When the polymer concentration was reduced to 5 mg/mL, relatively fewer cells were found to be growing on the film (Figure 8(a)), and all the attached cells did not assume their normal spread morphology. When the polymer concentration was increased to 10 mg/mL, cell attachment was enhanced and cells started to take on the expected morphology (Figure

8(b)). At 15 mg/mL, the highest number of cells was found and they showed extensive spreading on the films (Figure 8(c)). However, this trend did not continue when the polymer concentration was increased to 20 mg/mL, as the number of cells attached decreased (Figure 8(d)). The results from WST-1 proliferation assay support these observations. Generally, the cellular proliferative activity of HUVECs increased with increasing PU concentration from 5 mg/mL to 15 mg/mL, as evidenced by the approximately two-fold increase in the absorbance values as compared to the 5mg/mL group. A reversal of trend was observed when PU concentration was increased to 20 mg/mL, where the cell proliferative activity decreased, as evidenced by the consistently lower absorbance values as compared to the PU-POSS-15% group from day 1 to day 7. Interestingly, the PU-POSS-15% group also consistently showed a comparable level of cellular proliferative activity to that of the positive control group, which consists of polystyrene (PS) films. PS is a common material used to make the various cell culture vessels. This finding of the effect of pore size on cellular behaviors is in agreement with the results of a previous study [51]. An increasing polymer concentration corresponds to a smaller average pore size, which in turn enhances endothelial cell growth, albeit up to a certain limit. In addition, to contrast the good cytocompability of POSS molecules as an additive, another stabilizer known as pluronic F127 was used to produce PU-pluronic films at a PU concentration of 15 mg/mL (Figure 8(f)) via the BF method [53]. Upon the seeding of HUVECs, the cells were shown to attach and proliferate better on PU/POSS films as compared to PU-pluronic films.

4 Conclusions

This study describes the synthesis of highly ordered, honeycomb microstructured gelatin-grafted PU/POSS films. The incorporation of POSS nanostructured molecules and surface modifications through BF method and the subsequent biomacromolecule immobilization were shown to have a positive effect on improving the endothelium regeneration *in vitro* as evidenced by the presence of viable HUVECs on the film surface. Hence, it can be concluded that this is a promising way to enhance cell–material interaction on PU-based vascular grafts, ensuring a higher efficiency for endothelizations.

The work was financially supported by the National Natural Science Foundation of China (21376054), the Educational Commission of Zhejiang Province of China (Y201223742) and the AcRF Tier 1 Grant RG 36/12, Ministry of Education, Singapore.

1 Roger VL. Heart disease and stroke statistics-2012 update: A report from the American heart association. *Circulation*, 2012, 125: e2–e220
2 Nieponice A, Soletti L, Guan J, Deasy BM, Huard J, Wagner WR, Vorp DA. Development of a tissue-engineered vascular graft combining a biodegradable scaffold, muscle-derived stem cells and a rotational vacuum seeding technique. *Biomaterials*, 2008, 29: 825–833
3 Saitow C, Kaplan DL, Castellot Jr JJ. Heparin stimulates elastogenesis: application to silk-based vascular grafts. *Matrix biol*, 2011, 30: 346–355
4 Wang DA, Ji J, Sun YH, Yu GH, Feng LX. Blends of stearyl poly(ethylene oxide) coupling-polymer in chitosan as coating materials for polyurethane intravascular catheters. *J Biomed Mater Res*, 2001, 58: 372–383
5 Wang DA, Ji J, Gao CY, Yu GH, Feng LX. Surface coating of stearyl poly(ethylene oxide) coupling-polymer on polyurethane guiding catheters with poly(ether urethane) film-building additive for biomedical applications. *Biomaterials*, 2001, 22: 1549–1562
6 Harris JR, Seikaly H. Evaluation of polytetrafluoroethylene micrografts in microvascular surgery. *J Otolaryngol*, 2002, 31: 89–92
7 Kannan RY, Salacinski HJ, Butler PE, Hamilton G, Seifalian AM. Current status of prosthetic bypass grafts: a review. *J Biomed Mater Res B Appl Biomater*, 2005, 74: 570–581
8 Santerre JP, Woodhouse K, Laroche G, Labow RS. Understanding the biodegradation of polyurethanes: from classical implants to tissue engineering materials. *Biomaterials*, 2005, 26: 7457–7470
9 Wang DA, Ji J, Feng LX. Surface analysis of poly(ether urethane) blending stearyl polycethylene oxide coupling polymer. *Macromolecules*, 2000, 33: 8472–8478
10 Wang DA, Ji J, Feng LX. Various-sized stearyl poly(ethylene oxide) coupling-polymer blending poly(ether urethane) material for surface study and biomedical applications. *Macromol Chem Phys*, 2000, 201: 1574–1584
11 Fields C, Cassano A, Allen C, Meyer A, Pawlowski KJ, Bowlin GL, Rittgers SE, Szycher M. Endothelial cell seeding of a 4-mm I.D. Polyurethane vascular graft. *J Biomater Appl*, 2002, 17: 45–70
12 Lin HB, Sun W, Mosher DF, García-Echeverría C, Schaufelberger K, Lelkes PI, Cooper SL. Synthesis, surface, and cell-adhesion properties of polyurethanes containing covalently grafted RGD-peptides. *J Biomed Mater Res*, 1994, 28: 329–342
13 Kannan RY, Salacinski HJ, Butler PE, Seifalian AM. Polyhedral oligomeric silsesquioxane nanocomposites: the next generation material for biomedical applications. *Acc Chem Res*, 2005, 38: 879–884
14 Ghanbari H, de Mel A, Seifalian AM. Cardiovascular application of polyhedral oligomeric silsesquioxane nanomaterials: a glimpse into prospective horizons. *Int J Nanomedicine*, 2011, 6: 775–786
15 Wang DA, Feng LX, Ji J, Sun YH, Zheng XX, Elisseeff JH. Novel human endothelial cell-engineered polyurethane biomaterials for cardiovascular biomedical applications. *J Biomed Mater Res A*, 2003, 65A: 498–510
16 Wang DA. Engineering blood-contact biomaterials by "H-bond grafting" surface modification. *Adv Polym Sci*, 2007, 179–227
17 Widawski G, Rawiso M, François B. Self-organized honeycomb morphology of star-polymer polystyrene films. *Nature*, 1994, 369: 387–389
18 François B, Pitois O, François J. Polymer films with a self-organized honeycomb morphology. *Adv Mater*, 1995, 7: 1041–1044
19 Schuler M, Owen GR, Hamilton DW, de Wild M, Textor M, Brunette DM, Tosatti SG. Biomimetic modification of titanium dental implant model surfaces using the RGDSP-peptide sequence: a cell morphology study. *Biomaterials*, 2006, 27: 4003–4015
20 Wang DA, Ji J, Sun YH, Shen JC, Feng LX, Elisseeff JH. *In situ* immobilization of proteins and RGD peptide on polyurethane surfaces via poly(ethylene oxide) coupling polymers for human endothelial cell growth. *Biomacromolecules*, 2002, 3: 1286–1295
21 Martins MC, Wang D, Ji J, Feng L, Barbosa MA. Albumin and fibrinogen adsorption on Cibacron blue F3G-A immobilised onto PU-PHEMA (polyurethane-poly (hydroxyethylmethacrylate)) surfaces. *J Biomater Sci Polym Ed*, 2003, 14: 439–455

22 Martins MC, Wang D, Ji J, Feng L, Barbosa MA. Albumin and fibrinogen adsorption on PU-PHEMA surfaces. *Biomaterials*, 2003, 24: 2067–2076
23 Wang DA, Chen BL, Ji J, Feng LX. Selective adsorption of serum albumin on biomedical polyurethanes modified by a poly(ethylene oxide) coupling-polymer with Cibacron Blue (F3G-A) endgroups. *Bioconjug Chem*, 2002, 13: 792–803
24 Wang DA, Ji J, Feng LX. Selective binding of albumin on stearyl poly(ethylene oxide) coupling polymer-modified poly(ether urethane) surfaces. *J Biomater Sci Polym Ed*,2001, 12: 1123–1146
25 Lai Y, Xie C, Zhang Z, Lu W, Ding J. Design and synthesis of a potent peptide containing both specific and non-specific cell-adhesion motifs. *Biomaterials*, 2010, 31: 4809–4817
26 Zhu Y, Gao C, He T, Shen J. Endothelium regeneration on luminal surface of polyurethane vascular scaffold modified with diamine and covalently grafted with gelatin. *Biomaterials*, 2004, 25: 423–430
27 Liu W, Liu R, Li Y, Wang W, Ma L, Wu M, Huang Y. Self-organized ordered microporous thin films from grafting copolymers. *Polymers*, 2009, 50: 2716–2726
28 Xiong XP, Lin MF, Zou WW. Honeycomb structured porous films prepared by the method of breath figure: history and development. *Curr Org Chem*, 2011, 15: 3706–3718
29 Roohpour N, Wasikiewicz JM, Moshaverinia A, Paul D, Grahn MF, Rehman IU, Vadgama P. Polyurethane membranes modified with isopropyl myristate as a potential candidate for encapsulating electronic implants: a study of biocompatibility and water permeability. *Polymers*, 2010, 2: 102–119
30 Yabu H, Shimomura M. Single-step fabrication of transparent superhydrophobic porous polymer films. *Chem Mater*, 2005, 17: 5231–5234
31 Dong R, Ma H, Yan J, Fang Y, Hao J. Tunable morphology of 2D honeycomb-patterned films and the hydrophobicity of a ferrocenyl-based oligomer. *Chem Eur J*, 2011, 17: 7674–7684
32 Li L, Zhong YW, Chen CK, Li J. A novel path to patterning based on the static breath figure technique. *Acta Physico-Chimica Sinica*, 2010, 26: 1135–1142
33 Qin S, Li H, Yuan WZ, Zhang Y. Fabrication of polymeric honeycomb microporous films: breath figures strategy and stabilization of water droplets by fluorinated diblock copolymer micelles. *J Mater Sci*, 2012, 47: 6862–6871
34 Zhu Y, Sheng R, Luo T, Li H, Sun J, Chen S, Sun W, Cao A. Honeycomb-structured films by multifunctional amphiphilic biodegradable copolymers: surface morphology control and biomedical application as scaffolds for cell growth. *ACS Appl Mater Interfaces*, 2011, 3: 2487–2495
35 François B, Pitois O, François J. Polymer films with a self-organized honeycomb morphology. *Adv Mater*, 1995, 7: 1041–1044
36 Sharma V, Song LL, Jones RL, Barrow MS, Williams R, Srinivasarao M. Effect of solvent choice on breath-figure-templated assembly of "holey" polymer films. *EPL*, 2010, 91: 38001
37 Ferrari E, Fabbri P, Pilati F. Solvent and substrate contributions to the formation of breath figure patterns in polystyrene films. *Langmuir*, 2011, 27: 1874–1881
38 Park MS, Joo W, Kim JK. Porous structures of polymer films prepared by spin coating with mixed solvents under humid condition. *Langmuir*, 2006, 22: 4594–4598
39 Peng J, Han YC, Yang YM, Li BY. The influencing factors on the macroporous formation in polymer films by water droplet templating. *Polymer*, 2004, 45: 447–452
40 Beysens D, Steyer A, Guenoun P, Fritter D, Knobler CM. How does dew form? *Phase Transitions*, 1991, 31: 219–246
41 Xu Y, Zhu B. A study on formation of regular honeycomb pattern in polysulfone film. *Polymer*, 2005, 46: 713–717
42 Lin DT, Young TH, Fang Y. Studies on the effect of surface properties on the biocompatibility of polyurethane membranes. *Biomaterials*, 2001, 22: 1521–1529
43 Freij-Larsson C, Jannasch P, Wesslen B. Polyurethane surfaces modified by amphiphilic polymers: Effects on protein adsorption. *Biomaterials*, 2000, 21: 307–315
44 De Wael K, Verstraete A, Van Vlierberghe S, Dejonghe W, Dubruel P, Adriaens A. The electrochemistry of a gelatin modified gold electrode. *Int J Electrochem Sci*, 2011, 6: 1810–1819
45 Ren ZY, Wu HP, Ma JM, Ma DZ. FTIR studies on the model polyurethane hard segments based on a new waterborne chain extender dimethylol butanoic acid (DMBA). *Chin J Polym Sci*, 2004, 22: 225–230
46 Lim HR, Baek HS, Lee MH, Woo YI, Han DW, Han MH, Baik HK, Choi WS, Park KD, Chung KH, Park JC. Surface modification for enhancing behaviors of vascular endothelial cells onto polyurethane films by microwave-induced argon plasma. *Surf Coat Technol*, 2008, 202: 5768–5772
47 Guan J, Gao C, Feng L, Sheng J. Surface photo-grafting of polyurethane with 2-hydroxyethyl acrylate for promotion of human endothelial cell adhesion and growth. *J Biomater Sci Polym Ed*, 2000, 11: 523–536
48 Guan J, Gao C, Feng L, Shen J. Preparation of functional poly(ether-urethane) for immobilization of human living cells. 1. Surface graft polymerization of poly(ether-urethane) with 2-(dimethyl-amino)ethyl methacrylate and quaternization of grafted membrane. *Eur Polym J*, 2000, 36: 2707–2713
49 Guan J, Gao C, Feng L, Shen J. Surface modification of polyurethane for promotion of cell adhesion and growth 1: Surface photo-grafting with *N*,*N*-dimethylaminoethyl methacrylate and cytocompatibility of the modified surface. *J Mater Sci Mater Med*, 2001, 12: 447–452
50 Uttayarat P, Toworfe GK, Dietrich F, Lelkes PI, Composto RJ. Topographic guidance of endothelial cells on silicone surfaces with micro- to nanogrooves: orientation of actin filaments and focal adhesions. *J Biomed Mater Res Part A*, 2005, 75: 668–680
51 Narayan D, Venkatraman SS. Effect of pore size and interpore distance on endothelial cell growth on polymers. *J Biomed Mater Res Part A*, 2008, 87: 710–718
52 Lien SM, Ko LY, Huang TJ. Effect of pore size on ECM secretion and cell growth in gelatin scaffold for articular cartilage tissue engineering. *Acta Biomater*, 2009, 5: 670–679
53 Amirkhani M, Berger N, Abdelmohsen M, Zocholl F, Gonçalves MR, Marti O. The effect of different stabilizers on the formation of self-assembled porous film via the breath-figure technique. *J Polym Sci Part B*: *Polym Phys*, 2011, 49: 1430–1436